ALMA MATER STUDIORUM – UNIVERSITY OF BOLOGNA

SCHOOL OF ENGINEERING

DEPARTMENT of

ELECTRICAL, ELECTRONIC and INFORMATION ENGINEERING

"Guglielmo Marconi"

DEI

MASTER'S DEGREE IN TELECOMMUNICATIONS ENGINEERING

MASTER'S THESIS

in

Antennas for Wireless Systems

Numerical Investigation on Flat-Top Beam Arrays for Wireless Power Transfer in the Millimeter-Wave Range

Candidate:

Waleed Lodhi

Supervisor:

Prof. Diego Masotti

Co- Supervisor:

Engr. Enrico Fazzini

Academic Year

2021/2022

Contents

1. Introduction

The practice of sending electrical energy wirelessly from a power source to an electrical load is known as wireless power transfer (WPT). This can be achieved using electromagnetic waves, such as radio waves or microwaves, or using magnetic fields, such as induction. WPT has the potential to revolutionize the way electronic devices are powered and create new possibilities for energy transfer and distribution. WPT at mm-Wave range has the potential to offer several benefits, most of all improved energy efficiency compared to traditional WPT systems. It could also enable new applications, such as wireless charging of electric vehicles and powering of remote sensors and other devices in hard-to-reach locations.

The concept of WPT has been introduced around since the mid-17th century. As the name implies, the purpose of WPT is to transfer electrical power from a source to a device without the use of wires. The first WPT tests were carried out by Nikola Tesla, the inventor of AC power. His initial attempt to remotely light gas discharge lamps from more than 25 miles away was successful. His concept assumed that the earth is a conductor that can carry a charge throughout its entire surface. Although Tesla's idea of a proper WPT system was never properly funded, his initial research sparked the scientific world into a whole new era of power generation.

Today portable devices are a part of daily life. Most frequently used devices no longer need a constant power supply from the source. But the problem is that nearly all portable devices possess a battery, meaning, they all must be recharged using a wired charger. A mobile phone, PDA, digital camera, voice recorder, mp3 player, or laptop might now receive its power wirelessly—quite literally, "out of thin air" - instead of having to plug it in to recharge.

WPT is typically divided into two categories due to the mechanisms of energy transmission:

1. Far-field power transfer, also known as the radiative method
2. Near-field power transfer, also known as the non-radiative method

A detailed classification of wireless power transfer systems is shown in Figure 1.1 below. It can be seen from the figure, systems that transmit energy using microwaves are known as microwave power transfer (MPT), and those exploiting laser technology are known as laser power transfer (LPT). In turn, near-field wireless power transfer systems are split into two groups: capacitive power transfer (CPT), which uses an electric field to transfer energy, and inductive power transfer (IPT), which uses a magnetic field. Additionally, the transmission of energy using IPT can be realized with one of two technologies: coupled wireless power transfer (CWPT), or magnetically coupled resonance wireless power transfer (MCRWPT).

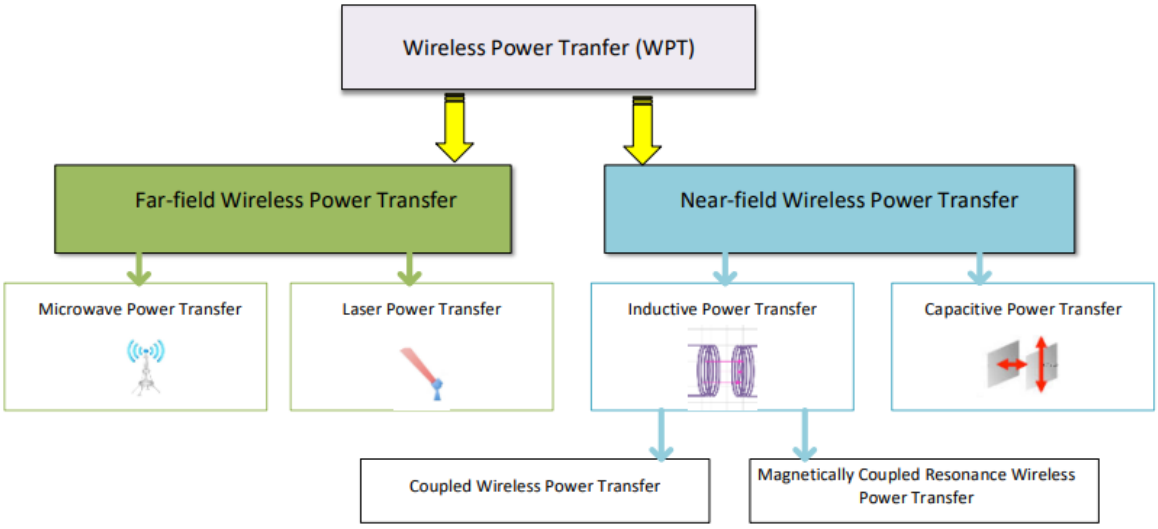

Figure 1.1 Classification of wireless power transfer [1]

Parameter	MCR WTP	IWPT	CTP
Frequency	Very high	High	Medium
Hysteresis losses	None	Appear	Appear
Eddy current losses	High	Medium	Low
Coupling factor	<0.25	>0.5	~1
Efficiency	Medium	High	Medium
Distance	Medium	Medium	Low

Table 1. Comparison of parameters of various IPT technologies [1]

Wireless power transfer system efficiency refers to the amount of electrical energy that is transferred wirelessly from a power source to a device or load, relative to the amount of energy that is input to the system. It is typically expressed as a percentage and is a measure of the effectiveness of the wireless power transfer system. Figure 1.2 shows the efficiencies of the wireless energy transfer systems depending on the distance between the transmitter and the receiver for both the near-field and far-field power transfer.

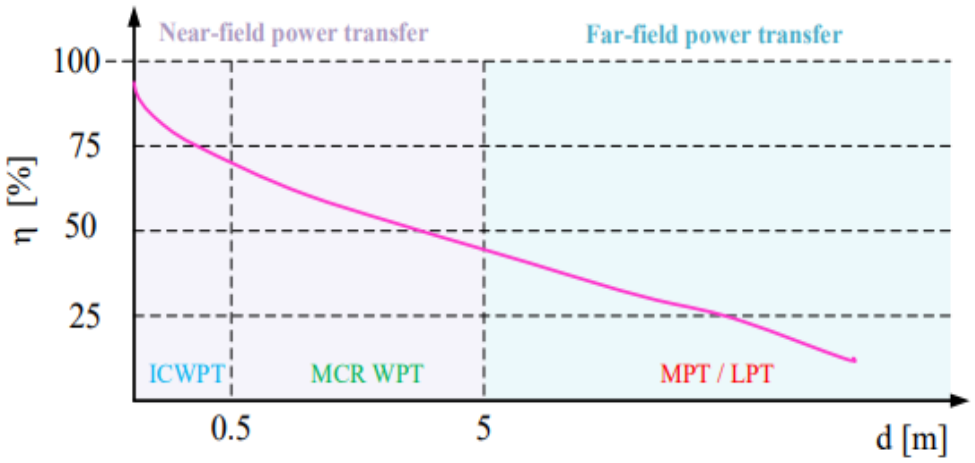

Figure 1. 2 Efficiency of wireless energy-transfer systems depending on the distance between the transmitter and the receiver [1].

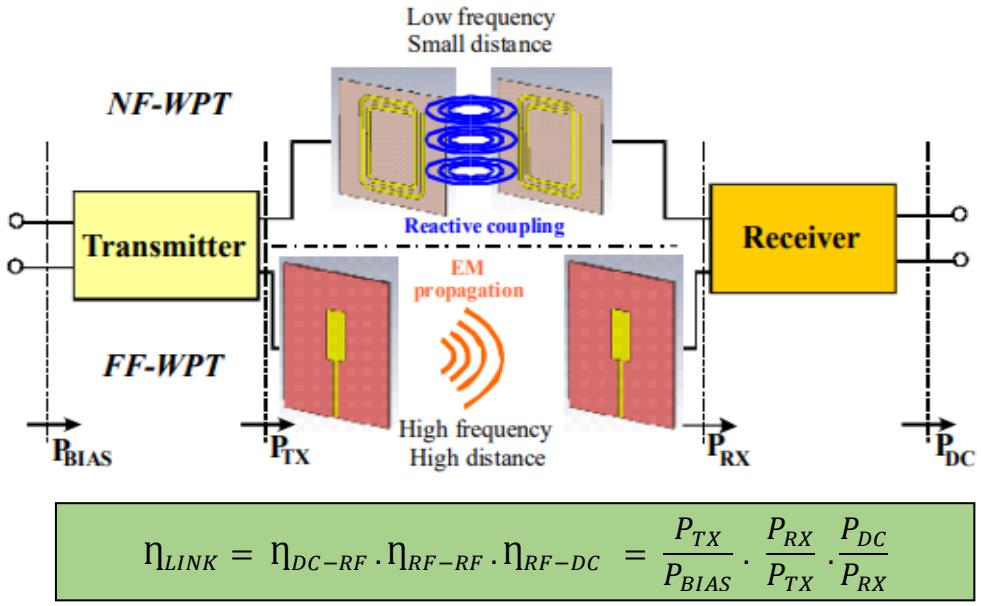

Figure 1.3 Efficiency of the Wireless Power Transfer System [2]

Figure 1.3 shows the total efficiency of WPT system, both for near and far field scenario, where three main terms can be individuated: η_{DC-RF} = DC to RF conversion efficiency, η_{RF-RF} = RF to RF efficiency (related to the wireless link) and η_{RF-DC} = RF to DC conversion efficiency. While for the first and the third term optimum results have been reached, the main bottleneck is represented by the link efficiency, where the isotropic attenuation doesn't allow to transfer great quantity of power, especially if mm-Wave is considered.

When looking at WPT, the normal use of charging small electrical devices has no adverse effects on the environment. WPT on a huge scale has been projected to produce only twenty grams of carbon dioxide- the worst cause of global warming- per kilowatt hour. Compared to

oil, which releases 846 grams of carbon dioxide per kilowatt hour, this is substantially less. While WPT and nuclear energy both produce emissions, WPT does not produce any radioactive waste that is detrimental to the environment. There is also a growing interest in WPT's potential applications, such as powering and charging mobile devices, electric vehicles (EVs), remote sensors and medical devices. This has led to the development of new prototypes and demonstration systems that show the potential of WPT.

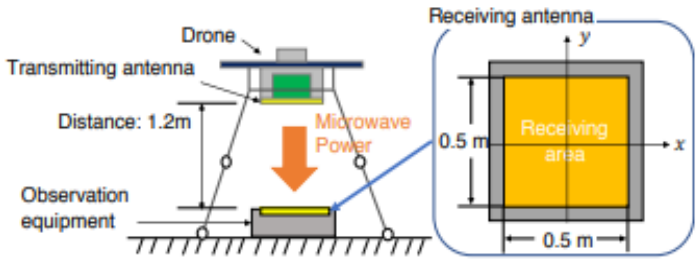

Figure 1. 4 The overview of microwave power supply by drone at volcanos [3]

There are uses for wireless power transfer in the medical industry as well. Using electrodes placed in the body, a pacemaker (an electrical device designed to stimulate regular heartbeat) has an average lifespan of five to eight years. If the power to the pacemaker is provided wirelessly there is no need to have an open-heart surgery after every five to eight years. Any electronic medical gadget inserted into a person can use this.

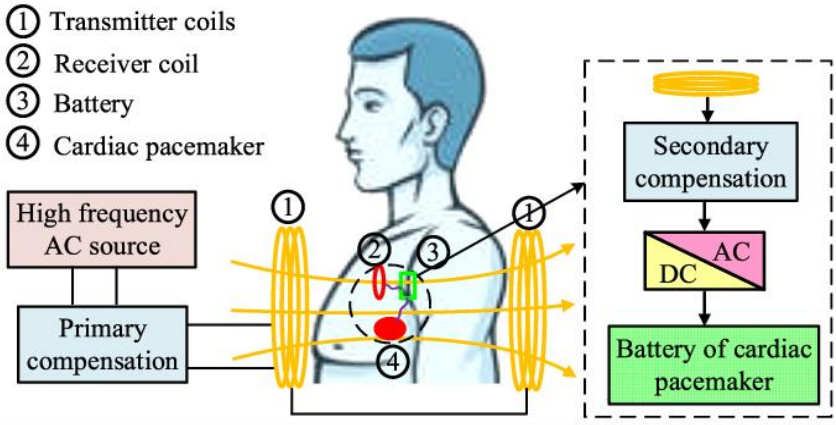

Figure 1. 5 Sandwiched implanted medical WPT system [4]

The main aim of this thesis assignment was the analysis of a far-field WPT link at mm-Wave, where the transmitter is a 10x10 planar dipole antenna array operating at 31 GHz that radiates 'flat-top beam', for which multiple excitation configurations were employed to optimize the flat-top beam radiated by the antenna array. The received system in the proposed link is

composed by a collection of single patch antennas distributed in space such that they cover the entire area invested by the flat radiation. The system in reception can be seen as a DC combiner, in fact each patch has its own rectifier circuit able to collect the RF power and transform into DC. Successively, all the DC contributions was summed for comparing the RF to DC efficiency of the entire mm-Wave for different flat top configurations.

The flat-top beam pattern is often used in applications where a high-gain directional antenna is required for long-range communication, but where the antenna needs to have a wide horizontal coverage area. Examples of such applications include point-to-point microwave links, terrestrial TV broadcasting, and radar systems. The flat-top antenna beam plays a crucial role in the efficiency of the wireless power transfer system, as it determines the directionality and shape of the electromagnetic field that is used to transfer power wirelessly.

The thesis was divided in the following phases:

a) Literature review

b) Understanding of the software

c) Antenna array design

d) Flat-top beam design

e) Flat-top beam optimization

f) Computation of the area invested by the beam, estimation of patch antennas required to cover that area and finally

g) Estimation of the total RF-DC efficiency for the entire system

In chapter 2, the antenna terminologies and an overall concept of the antenna arrays will be described. Chapter 3 explains flat-top beam in general and is based on the antenna array design phase and the implementation of the flat-top beam in two configurations, as well as the simulation results. Chapter 4 focuses on the receiver side and contains the numerical analysis to estimate the number of patch antennas to fill the area invested by the beam and the estimation of RF-DC efficiency. Finally, in chapter 5 all the numerical analysis results related to received power and RF-DC efficiency are compiled and compared.

2. Antenna's theory

An antenna is a device that either radiates energy in response to an applied source excitation or receives radiation due to an external electromagnetic field. When it is in transmitting mode, an excitation applied to the antenna terminals produces a current on the antenna. This current radiates, inducing electromagnetic fields in the region surrounding the antenna. The EM fields are easiest to analyze in the far-field region where angular variation of the radiation fields is independent of the radial distance. While there is no concrete theoretical definition of the far field region but commonly, the far field is the region beyond radial distance R, where R satisfies the following criterions [5].

$$R > D$$
$$R > \lambda$$
$$R > 2D^2/\lambda$$

Where D is the largest dimension of the antenna. Generally, especially in the field of wireless communications, antennas and wavelengths are small enough that we can surely assume the far-field condition holds.
In the following section the most important parameters regarding the radiation properties of the antennas will be presented.

2.1 Antenna's properties

- **Radiated Power:** Radiated power by an antenna is the amount of electromagnetic energy that is transmitted by the antenna into a surrounding medium. The radiated power through a spherical surface S_r with its center in the phase center of the antenna and radius r is given by

$$P_T = \int_{Sr} \frac{||E(P)||^2}{2\eta}\, dS_r = \int_0^{2\pi}\int_0^{\pi} \frac{||E(P)||^2}{2\eta} r^2 sin\theta d\theta d\phi \qquad (1)$$

Where,

E = Electric Field

P = Poynting Vector

η = Intrinsic impedance of the medium

- **Power Density:** The power density is determined by the Poynting vector and is the radiated power per unit surface through a spherical surface S_r located in the far-field zone. It is given by eq. 2 and is measured in W/m^2.

$$\frac{dP_T}{dS_r} = p(r,\theta,\phi) = \frac{E(P)\ \mathrm{x}\ H^*(P)}{2}\ .\hat{r} = \frac{||E(r,\theta,\phi||^2}{2\eta} \qquad (2)$$

- **Radiation Intensity:** is defined as the radiated power per unit solid angle in a specific direction (θ,ϕ). It is obtained by simply multiplying the power density by the square of distance. The unit of radiation intensity is Watts/Steradian.

$$I_R(\theta,\phi) = p(r,\theta,\phi)r^2 = \frac{||E(r,\theta,\phi||^2}{2\eta}r^2 \qquad (3)$$

- **Directivity:** can be defined as the ratio of the actual power density (in a given direction) and the power density the antenna would have radiated if it was isotropic.

$$D(\theta,\phi) = \frac{p(r,\theta,\phi)}{\frac{P_T}{4\pi r^2}} = \frac{4\pi I_R(\theta,\phi)}{P_T} \qquad (4)$$

Note: D = 1 for the ideal isotropic radiator and D > 1 for a directional antenna. Where, the term $\frac{P_T}{4\pi r^2}$ = Average transmitted power on a sphere of radius r.

- **Radiation Efficiency:** The radiation efficiency of an antenna is a measure of the antenna's ability to convert the power that is fed into it into electromagnetic radiation that is transmitted into space. It is typically expressed in percentage.

$$\delta = \frac{P_T}{P_E} = \leq 1 \qquad (5)$$

Where, P_E is the mean power delivered by the transmitter to the antenna. Good antennas have $\delta = 80 - 95\%$.

- **Gain:** Antenna gain is a measure of how directionally selective an antenna is. However, gain also accounts for the fact that some energy is lost in the antenna itself. It is expressed in dBi as,

$$g(\theta,\phi) = \frac{4\pi I_R(\theta,\phi)}{P_E} = \delta_T\, D(\theta,\phi) \qquad (6)$$

- **Radiation Pattern:** The radiation pattern describes how the antenna radiates in space and it is a plot of the radiation function given by,

$$f(\theta,\phi) = \sqrt{\frac{I_R(\theta,\phi)}{I_R(\theta_m,\phi_m)}} \qquad (7)$$

  Where, $I_R(\theta_m,\phi_m)$ is the radiation intensity in maximum direction.

- **Reflection Coefficient and Matching Condition:** The reflection coefficient corresponds to the antenna port and is given by,

$$\rho_A = \frac{V_-}{V_+} \qquad (8)$$

  Where, V_- = Reflected voltage coefficient and V_+ = Forward voltage coefficient. It is very important to know that how the reflection coefficient is related to the antenna impedance (Z_A) and the characteristic impedance (Z_C) of the line. For perfect matching, $Z_A = Z_C$.

$$\rho_A = \frac{Z_A - Z_C}{Z_A + Z_C} \qquad (9)$$

2.2 Array Theory

An array is defined as a set of coherently fed radiating elements (antennas) arranged and excited in such a way as to produce a radiation pattern having prescribed properties.

Array theory involves mathematical analysis and design techniques to determine the optimal configuration of the antenna elements, such as their spacing, number, and phase relationships, in order to obtain desired radiation pattern based on the types of application. There are several types of arrays, depending for example on the geometry involved, as linear, circular, and planar arrays, each with their own unique characteristics and benefits. Array theory is a crucial area of study in modern antenna engineering, as it has numerous applications in areas such as wireless communication, radar, and remote sensing.

2.2.1 Uniform Arrays

Figure 2.1 illustrates an array of isotropic elements placed along the x-axis. The spacing between the elements is a constant d.

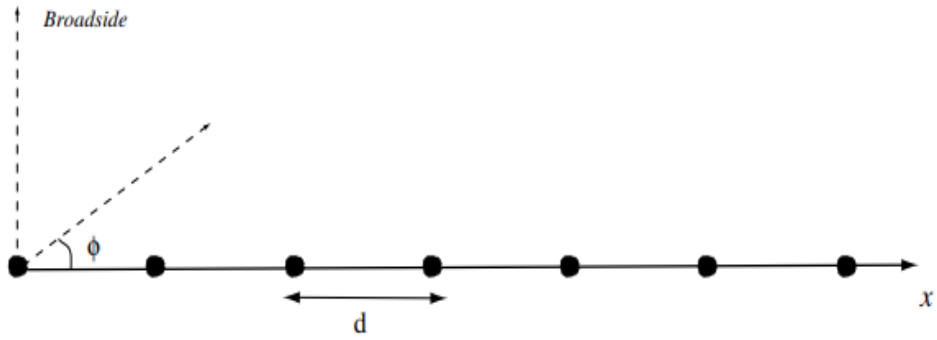

Figure 2.1 Orientation of a linear array

An array composed by identical elements uniformly excited and equally spaced is called uniform array. In this case, it can be stated that the radiation pattern can be evaluated as the product of the basis element pattern and the normalized array factor, restoring the principle of pattern multiplication.

The array factor is a function of the position and amplitude of each element in the array, and it describes the directionality and gain of the overall antenna system. In other words, the array factor represents the constructive and destructive interference of the signals emitted by the individual elements of the linear array, and it determines the direction and strength of the resulting signal and for uniform linear arrays is given by equation below.

The array factor is given by the following equation,

$$F(\theta, \phi) = \sum_{k=0}^{n-1} [e^{j(\beta L cos\Psi - \delta)}]^k \qquad (10)$$

Where u = auxiliary angular coordinate $= \frac{\pi}{\lambda} L \cos \Psi - \frac{\delta}{2}$, δ = inter-element phase delay, hence the above equation becomes,

$$F(\theta, \phi) = \sum_{k=0}^{n-1} [e^{j2u}]^k \qquad (11)$$

Where, n = number of elements and Ψ describes the direction of radiation.

a) Broadside Array:

It is preferable in many applications having an array whose maximum radiation points perpendicular with respect to the array axis. In this case, it is referred to as broadside array.

$$u = \frac{\pi}{\lambda} L \cos\Psi - \frac{\delta}{2} \qquad (12)$$

Selecting $\Psi = 90°$ and u = 0, gives $\delta = 0$ i.e., in-phase excitation meaning all the currents/signals feeding the n-elements of the uniform array are in phase. Another condition for the broadside array is that the spacing between the elements must be equal to λ/2 i.e., L = λ/2.

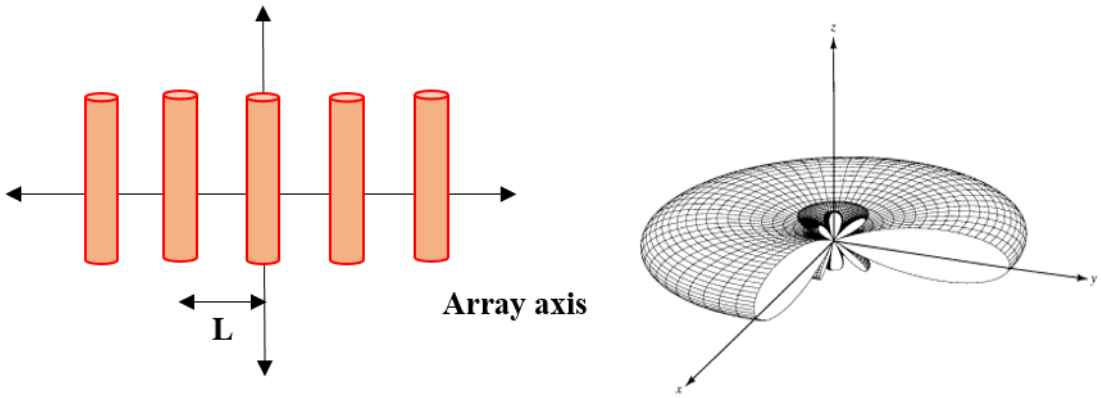

Figure 2.2 Broadside arrangement of antenna array on the left and its radiation pattern on right [5]

b) End-Fire Array:

Instead of having the maximum radiation broadside to the axis of the array, it may be desirable to direct it along the axis of the array (end-fire). As a matter of fact, it may be necessary that it radiates toward only one direction (either $\Psi = 0°$ or $180°$).

$$u = \frac{\pi}{\lambda} L \cos\Psi - \frac{\delta}{2}$$

Selecting u = 0 and $\Psi = 0$ in the above equation yields, $\delta = \beta L$, where $\beta = \frac{2\pi}{\lambda}$. The first condition to fulfil for the end-fire array is that the spacing between the elements must be equal

to λ/4 which leads to the second condition by putting L = λ/4 in δ = βL i.e. δ = π/2. Therefore to have an end-fire array, the spacing between the elements must be equal to λ/4 and all the currents/signals feeding the n-elements of the uniform array must be 90° out of phase.

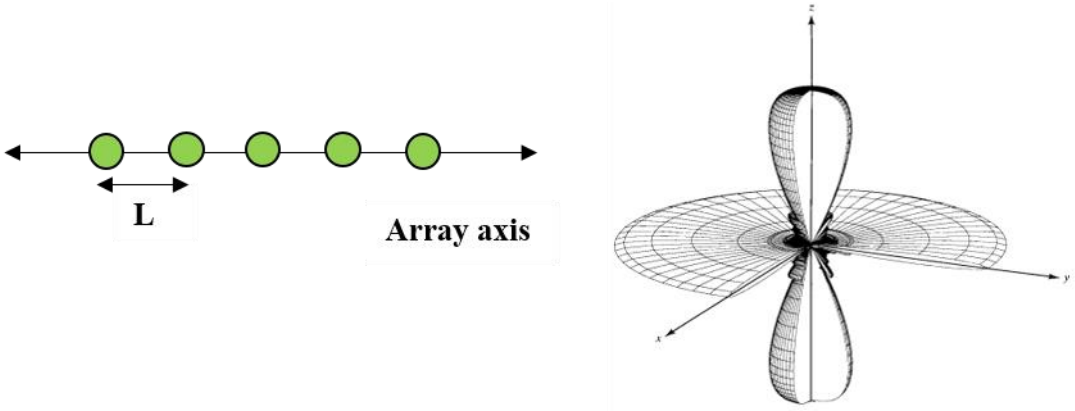

Figure 2.3 End-fire arrangement of antenna array on the left and its radiation pattern on right

c) Planar Array:

Individual radiators can be arranged along a rectangular grid to create a rectangular or planar array in addition to putting elements along a line (to produce a linear array). Planar arrays offer more variables that can be utilized to control and shape the array's pattern. Planar arrays are more adaptable and can produce patterns with lower side lobes that are more symmetrical [5]. In case of a planar array, there are two array factors, one along x and the other along y described through eq. 13.

$$F(\theta, \phi) = F(\theta, \phi)_x F(\theta, \phi)_y \qquad (13)$$

Figure 2.4 below shows a broadside uniform 2-dimensional array of half-wave dipoles arranged on the x-y plane. In this case the same conditions described previously would apply in two dimensions i.e., $d_x = L_x = \lambda/2$ and $\delta_x = \delta_y = 0$.

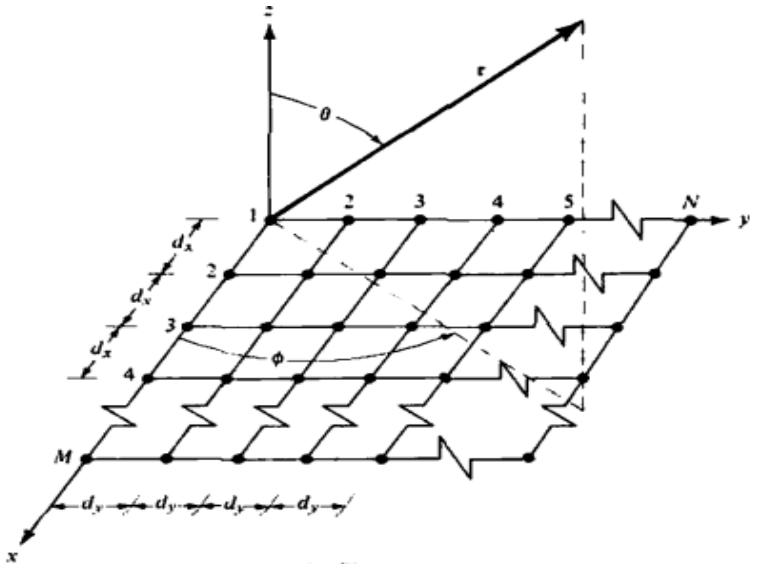

Figure 2.4 A general 2D planar array [5]

In a planar array, the radiation pattern becomes controllable not just in a single plane, as offered by linear solution, but the control is extended to 3D space in order to create precise and focused radiation as presented in Figure 2.5.

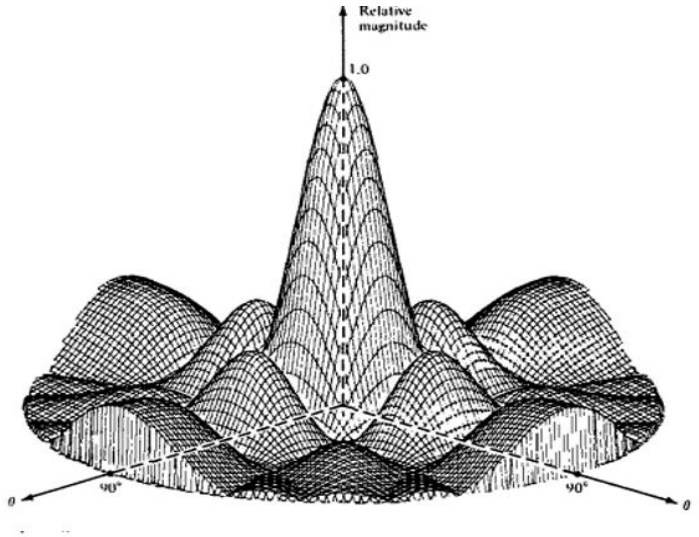

Figure 2.5 Three-dimensional antenna pattern of a planar array with spacing of $d_x = d_y = \lambda/2$

3. Design and Implementation of Flat-Top beam Array at 31 GHz

In this chapter the concept of flat-top beam radiators will be described and the method that can be exploited for its generation and optimization will be discussed.

3.1 Flat-Top Beam

A flat-top beam, also known as a top-hat beam, is a type of beam that has a flat and uniform intensity profile across its beam width, therefore showing a constant intensity across their entire width.

Flat-top beams are used in various applications such as material processing, medical treatments and wireless power transfer applications. Additionally, flat-top beams can be tailored to fit specific geometries and requirements, making them a versatile option in many different areas.

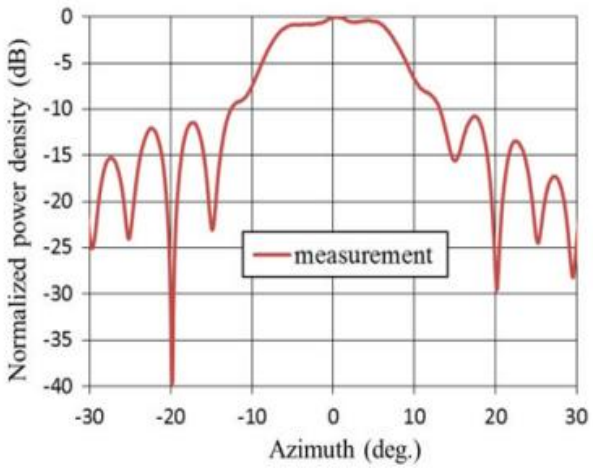

Figure 3.1 The measured beam pattern of the experiment performed in [6]

For what regards wireless power transfer systems, flat top beam radiators are implied to efficiently deliver power to a target device over a distance without the need for a direct physical connection in an extended area if compared with traditional uniform arrays. By using a flat top beam, the power can be transmitted over longer distances with minimal loss or interference, making it a popular choice for applications such as wireless charging for electric vehicles and other portable devices. Flat-topped beams can provide a uniform power density to the receiver in wireless power transmission, which is of great significance to improve the receiving efficiency and to simplify the design of rectifier circuit.

Compared to other types of beams, such as Gaussian beams, flat-top beams are less affected by diffraction and scattering, which can cause the energy to spread out and reduce the efficiency

of the power transfer. Additionally, flat-top beams can be shaped and focused more precisely, allowing for greater control over the direction and intensity of the power transfer. Overall, the use of flat-top beams in wireless power transfer can result in more efficient, reliable, and cost-effective charging solutions.

The design of a flat top beam architectures starts considering linear or bi-dimensional arrays for which the uniformity condition is not respected: in fact, even if the inter-element distance remains constant between two consecutive elements, the coherently feeding condition is violated since the amplitude of the signals radiated by the single elements are not equals for enhancing the width of the main beam.

Since the procedure of finding optimal amplitude and phase for the radiating signals is not immediate, usually optimization algorithm are exploited. In the following section a list of the most common optimizer is presented.

- Genetic Algorithm: A genetic algorithm is an optimization technique inspired by the principles of natural selection and evolution. It starts with a population of potential solutions, represented as individuals or "chromosomes" in a population. The genetic algorithm optimizes the flat-top beam by searching for the optimal set of parameters using a fitness function to evaluate the quality of each candidate solution. By iteratively applying genetic operators to the population, the algorithm can find the best solution that produces the optimal flat-top beam.
- Particle Swarm Optimization: One of the bio-inspired algorithms, particle swarm optimization (PSO), is straightforward in its search for the best solution in the problem space. PSO optimizes the flat-top beam by searching for the optimal set of parameters using a swarm of particles that adjust their velocity and position based on their best position so far and the best position found by the swarm. By iterating through these steps, the algorithm can find the best amplitudes and phases that produces the optimal flat-top beam.
- Woodward and Lawson Method: A very popular antenna pattern synthesis method used for beam shaping was introduced by Woodward and Lawson. The synthesis is accomplished by sampling the desired pattern at various discrete locations [5]. The Woodward and Lawson method takes a Gaussian beam and uses a phase shifter.

In this thesis work, we refer to an excitation set found through genetic algorithm from [7] that considers a linear array of wideband cross-polarized antenna composed by 10 elements.

The idea is to replicate the same structure involving the planar technology operating at 31 GHz and then design a bi-dimensional matrix array of 10x10 where the flat top beam excitation is developed in two different configurations.

3.2 Design of 10x10 Planar Dipole Array

The array was designed in the X-Y plane so that the direction of radiation is in the Z-direction. Rogers RO3003 having a thickness of 0.256 mm, that is a high-frequency circuit board material, was used as an antenna substrate and copper of 35 μm was used as the material for antenna. The spacing between the antenna elements is λ/2 in order to realize broadside radiation. As the working frequency is 31 GHz, results λ = 9.7 mm and then λ/2 comes out to be 9.7/2 = 4.84 mm. The λ/2 spacing between the antenna elements helps to minimize the mutual coupling resulting in maximum radiation efficiency for the array, it also avoids grating lobes, improves the directivity of the array. Since dipole antennas are used as single elements, a shield at distance $\frac{\lambda_0}{4}$ is inserted in order to eliminate the back radiation and having the far field just in positive Z-direction.

The table shown below contains all the parameters considered for the design and optimization of the 10x10 planar dipole array, while in figure 3.2 the prototype is shown.

Parameter	Dimension (mm)
Substrate Width	50
Substrate Length	50
Substrate thickness	0.256
Dipole Width	0.5
Dipole Length	3.20
Dipole Height	0.035
Dipole Gap	0.4
Gap Between Shield and Dipole	2.42

Table 2. Antenna Parameters

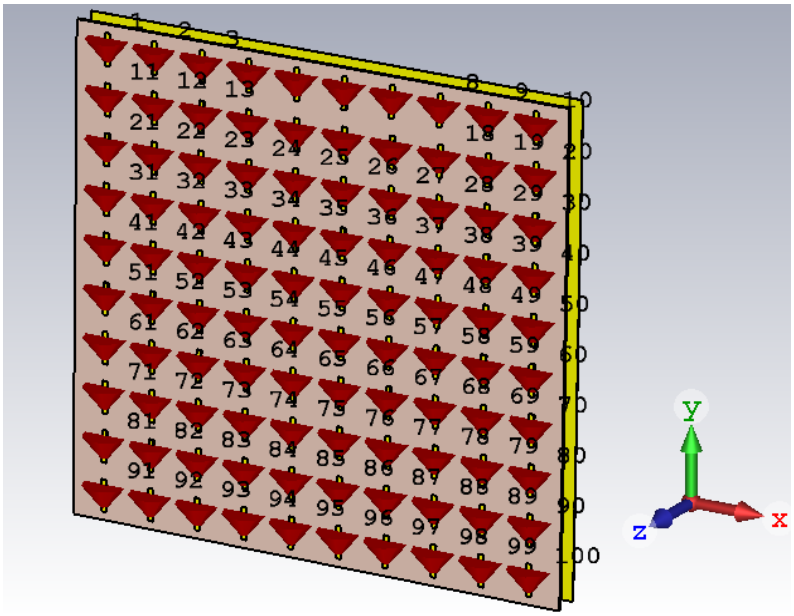

Figure 3.2 10x10 planar dipole array in the X-Y plane

3.3 Uniform Excitation

The first excitation configuration considered is uniform, in order to check the correctness of the geometry involved. Since the system is composed by 100 ports (one for each radiating elements), thanks to the post-processing tool offered by CST Studio Suite the several contributions can be collected creating the overall contribution, restituting therefore the array factor characteristics. So, in the post-processing stage every port is excited with a sinusoidal CW with amplitude = 1V. This means an average power of 0.5 W at every port. Summing all the contributions the total average radiated power can be easily retrieved, considering the array as composed by 10 rows each one containing 10 elements.

$$P_{AV}^{single\ port} = \left[\frac{(A)^2}{2}\right] = 0.5\ W = 27\ dBm \qquad (14)$$

$$P_{AV} = 10 \sum_{i=1}^{10} \left[\frac{(A)^2}{2}\right] = 50W = 47\ dBm$$

The far-field simulation is presented in the following figure in polar coordinates, showing an angular width (3dB) of 10.2°, a gain of 23.4 dB and an efficiency of 71% in both planes (phi =

0°, phi = 90°), while the reflection coefficient at each port is below – 10 dB, showing acceptable results at the interested frequency, as shown in Figure 3.5.

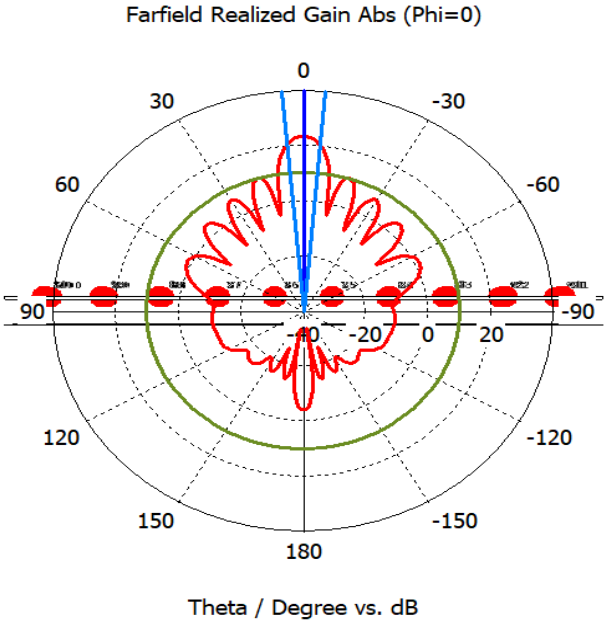

Figure 3.3 Far-field radiation pattern in polar coordinates for uniform excitation in phi =.0°

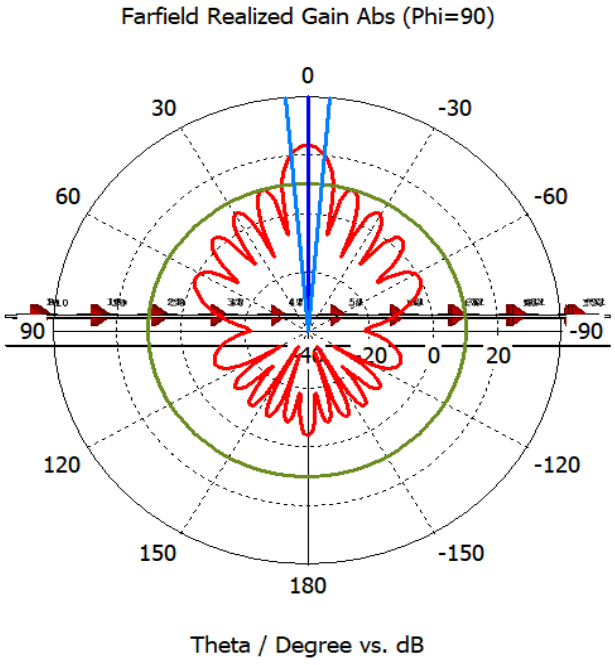

Figure 3.4 Far-field radiation pattern in polar coordinates for uniform excitation in phi = 90°

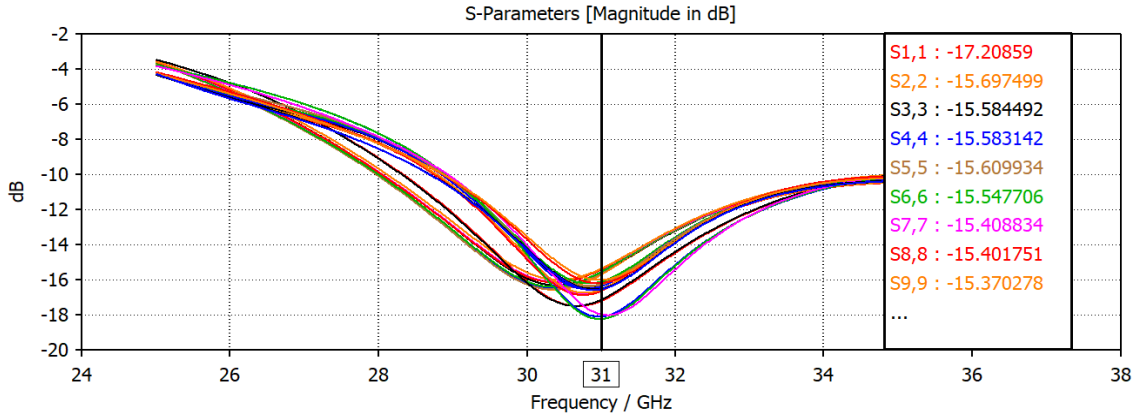

Figure 3.5 Reflection coefficients centered at resonance frequency.

3.4 Excitation for Flat-top Beam

As stated before, the excitation set for flat top beam characteristic is highlighted in [7] for linear configuration. It has been found through a genetic algorithm that modify the amplitude and phase of the radiated signal in order to control that their constructive interference creates a uniform amplitude over a wider area respect to the simple uniform excitation. Since in this thesis a planar bi-dimensional array is considered, 2 different configurations were considered.

3.4.1 Configuration 1 (Along Rows)

The first configuration applies the flat top excitation condition rows by rows. By using the amplitudes and phases described in figure 3.6, the flat-top beam was achieved.

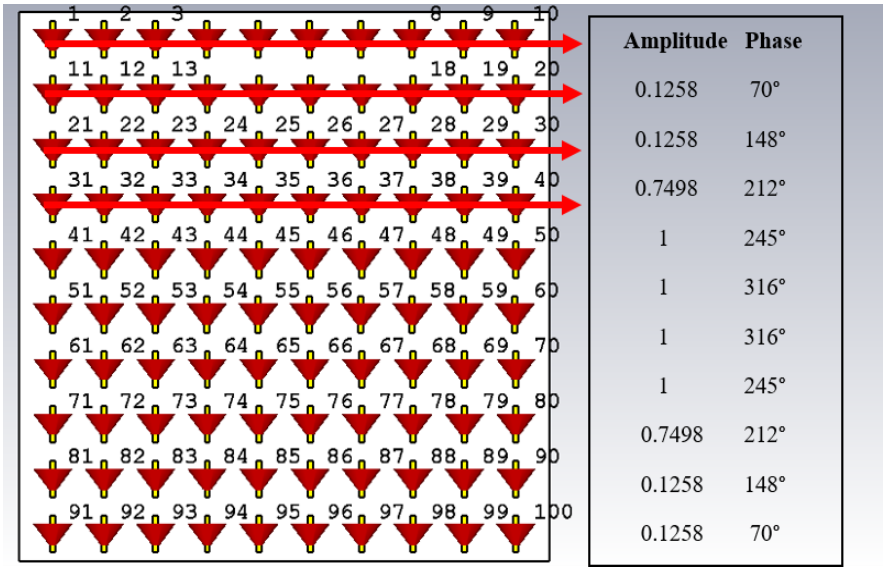

Figure 3.6 Amplitude and phase distribution along rows

From figure 3.6 the same set of amplitudes and phases were repeated row by row throughout the structure. Table 3 shows the average power corresponding to the excitations applied.

Port No.	Average Power (W)	Amplitude (V)	Phase (°)
1	0.0079	0.1258	70
2	0.0079	0.1258	148
3	0.2811	0.7498	212
4	0.5	1	245
5	0.5	1	316
6	0.5	1	316
7	0.5	1	245
8	0.2811	0.7498	212
9	0.0079	0.1258	148
10	0.0079	0.1258	70

Table 3. Excitation list to achieve flat- top beam.

The far-field simulation is presented in the following figures in polar coordinates, showing an angular width (3dB) of 27° and a gain of 17.8 dB in plane phi = 0°, while an angular width (3dB) of 10° in plane phi = 90°. The total efficiency was found to be 75 %.

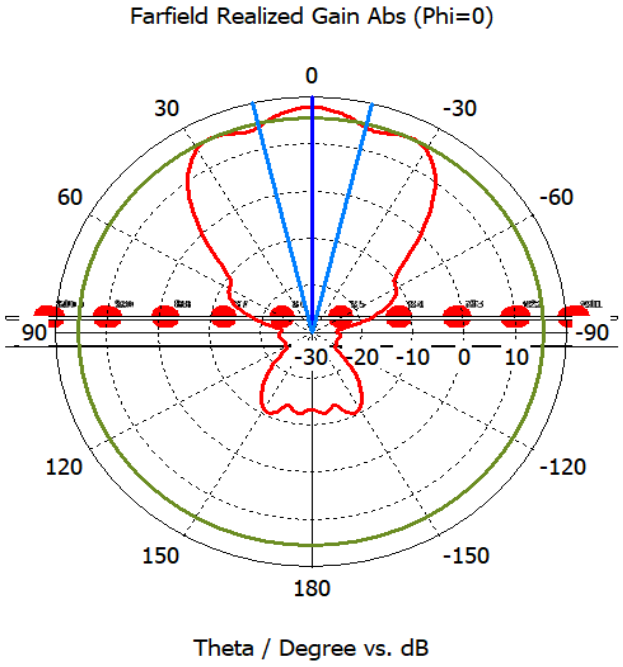

Figure 3.7 Far-field radiation pattern in polar coordinates for flat-top excitation in phi = 0

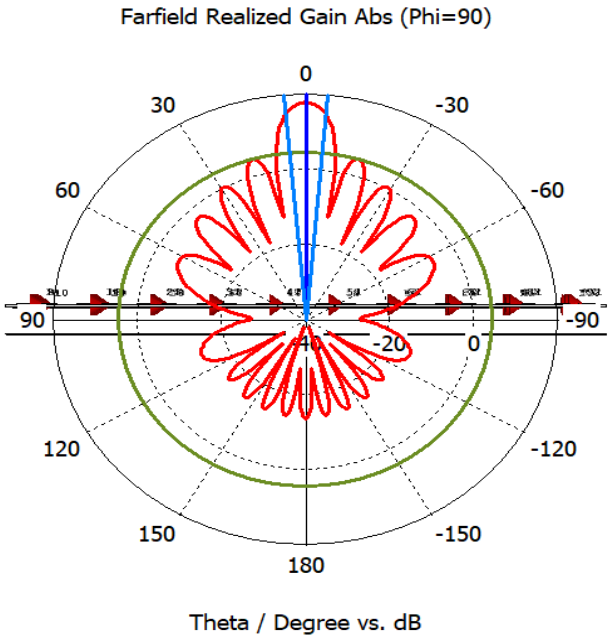

Figure 3.8 Far-field radiation pattern in polar coordinates for flat-top excitation in phi = 90°

It has been observed that the flatness can be improved by adjusting the amplitude of the central dipoles (reducing them) and were responsible for the extent of the flatness. On the other hand, changing these parameters means from one side increasing the flatness but from the other side means increasing the SLL values. Therefore, a trade-off must be found. Table 4 shows the amplitudes and phases applied to each row of antennas to improve the flatness and the far-field radiation pattern is presented in figure 3.9.

Port No.	Average Power (W)	Amplitude (W)	Phase
1	0.0079	0.1258	70
2	0.0079	0.1258	148
3	0.2811	0.7498	212
4	0.32	0.8	245
5	0.32	0.8	316
6	0.32	0.8	316
7	0.32	0.8	245
8	0.2811	0.7498	212
9	0.0079	0.1258	148
10	0.0079	0.1258	70

Table 4. Excitation list to improve the flatness

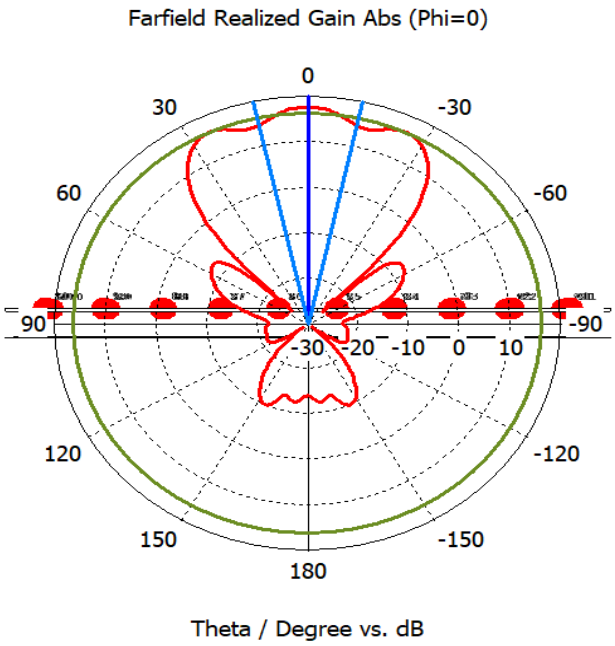

Figure 3.9 Far-field radiation pattern in polar coordinates showing improved flatness but a higher SLL in phi = 0°

The total average power can be computed in the same manner as previously presented and considering the values of table 3:

$$P_{AV} = 10 \sum_{i=1}^{10} \frac{(A)^2}{2} = 44\ dBm$$

3.4.2 Configuration 2D

In the configuration 2D, the amplitude and phases were applied in a 2-dimensional manner to achieve a 2D beam pattern, as shown in Figure 3.10., considering again the values of Table 3.

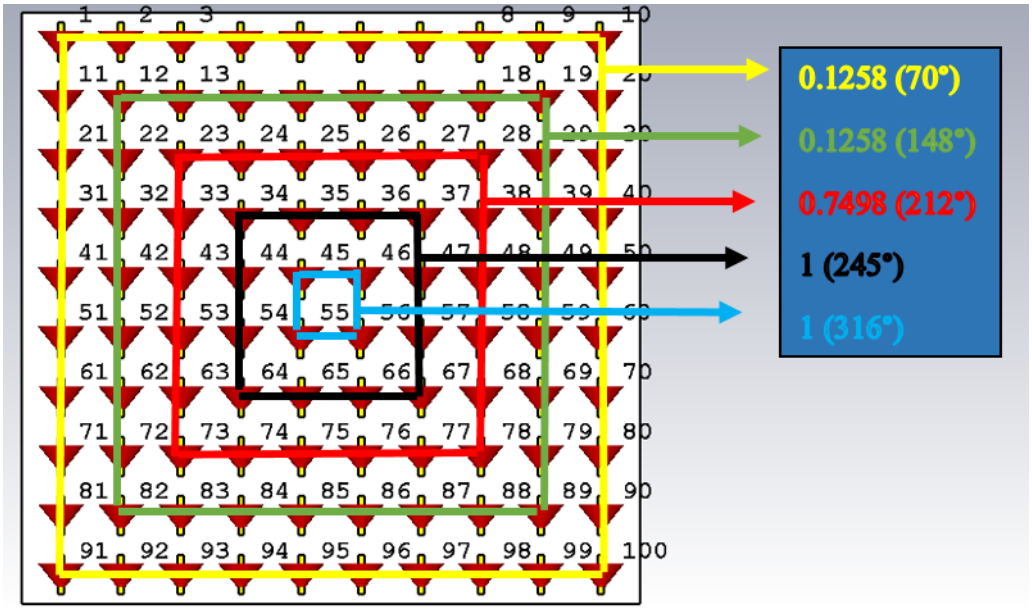

Figure 3.10 Amplitude and phase distribution in 2D

The main aim for the 2D configuration was to have a flat-top beam not just in one plane, but for $\varphi = 0°$ and $\varphi = 90°$. The total average power radiated by the array considering fig. 3.10 was calculated using the same expression and was found to be:

$$P_{AV} = 14W = 41dBm$$

The far-field simulation is shown in figure 3.11 and figure 3.12 in polar coordinates, which resulted in an angular width (3dB) of 23° in both planes (phi = 0° and phi = 90°) and a realized gain of 15.8 dB. The radiation efficiency was found to be 74%.

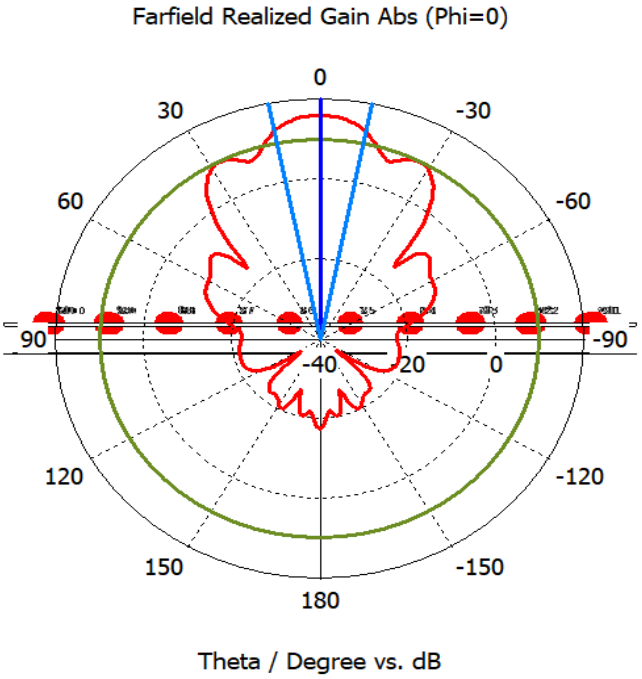

Figure 3.11 Far-field radiation pattern in polar coordinates for flat-top excitation in phi = 0° for configuration 2D

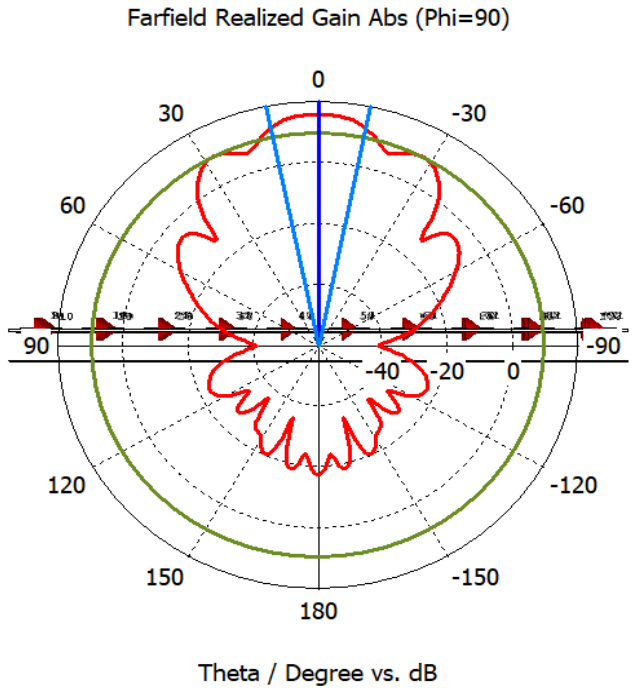

Figure 3.12 Far-field radiation pattern in polar coordinates for flat-top excitation in phi =90° for configuration 2D

Also, for configuration 2D, simulations were carried out to improve the flatness. The flatness was found to be better but the realized gain was reduced to 14 dB compared to 15.8 dB. Therefore, a trade-off must be found. The depiction shown in figure 3.13 presents that how the amplitudes and phases were applied and figure 3.14 shows the far-field radiation pattern.

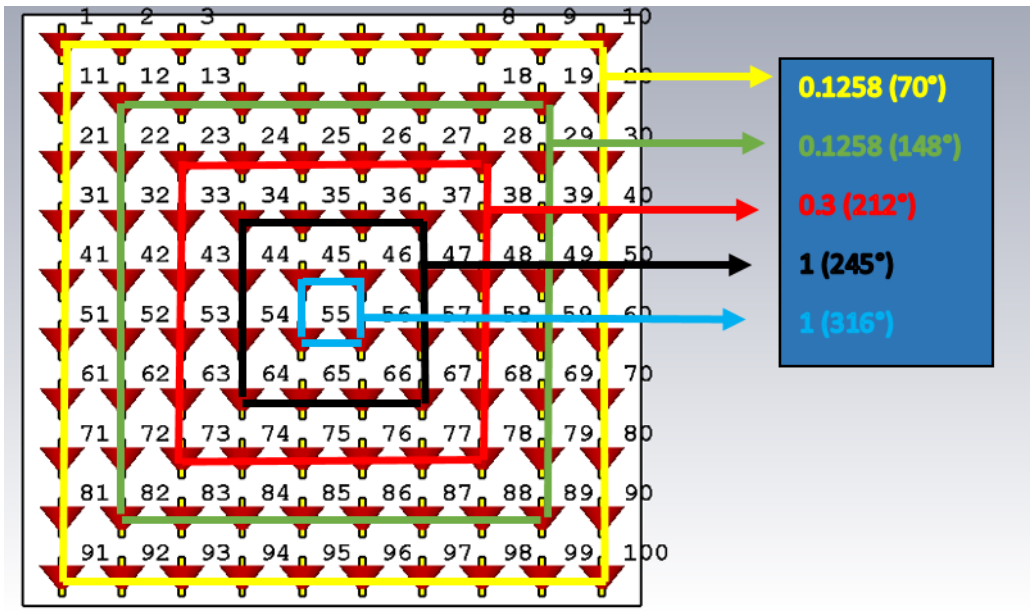

Figure 3.13 Amplitude and phase distribution in 2D to improve flatness

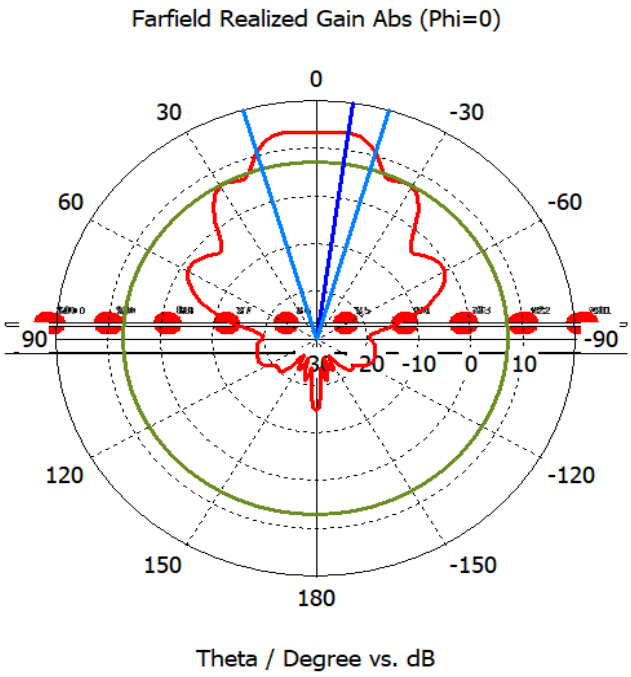

Figure 3.14 Far-field radiation pattern in polar coordinates to improve the flatness for configuration 2D.

4. Rectification Efficiency Estimation at Receiver Side

The process of transforming an alternating current (AC) signal into a direct current (DC) signal is known as rectification. This is accomplished by passing the AC signal through a rectifier, a device that only permits current to flow in one direction. There are two main types of rectifiers:

- **Half-wave rectifier:** Only one-half of the input waveform can pass through the circuit with this kind of rectifier. The diode is forward-biased and current flows through the load during the positive half-cycle. The diode is reverse-biased and the load is not conducting any current during the negative half-cycle. As a result, a half-wave rectifier produces a pulsating DC waveform with just half of the input signal.

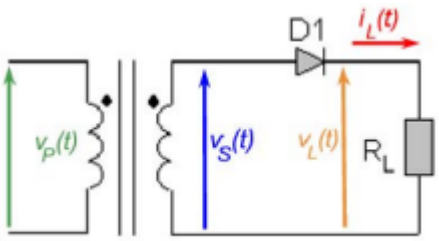

Figure 4.1 A half-wave rectifier [8]

- **Full-wave rectifier:** With this type of rectifier, current can move through the circuit during both the positive and negative halves of the input waveform. The bridge rectifier, which has four diodes stacked in a bridge arrangement, is the most popular kind of full-wave rectifier. The rectification takes place by the conduction of couples of diodes. Diodes D1 and D4 are conducting during the positive half-wave of the voltage. Diode D2 and D3 are conducting during the negative half. This is a double-way topology. In each half-cycle the current flows in both directions in the secondary winding but always in the same direction in the load. Compared to a half-wave rectifier, the output waveform of a full-wave rectifier is smoother and has less ripple.

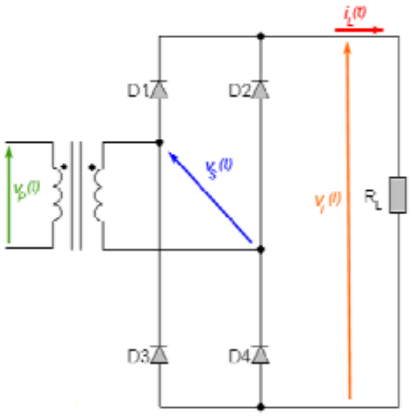

Figure 4.2 A full wave rectifier [8]

After accomplishing the flat-top beam in both the configurations, the next task was to estimate the rectification efficiency at the receiver side.

The rectenna system is composed by a receiving coaxial fed patch antenna, again restoring the planar technology, then followed by a voltage double rectifier, a special type of full wave rectifier. The size or area of the flat beam spot was measured using geometrical analysis for both the configurations at different distances, therefore it is filled by each rectenna system. The rectified DC power computed for each receiving system is then summed, composing the so-called DC combiner.

4.1 Design of Receiving Coaxial Fed Patch Antenna

The receiving antenna consists of a rectangular patch operating at 31 GHz and realized in copper 35 μm on a Rogers RO3003 substrate. As excitation technique, a coaxial feeding line is implemented.

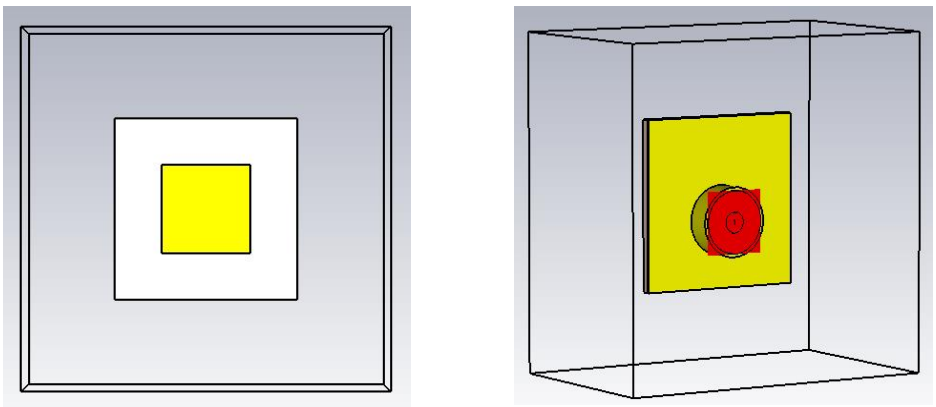

Figure 4.3 Coaxial Fed Patch Antenna

The list of parameters used for the simulation and their values are shown in the below table 5.

Parameter	Dimension (mm)
Substrate Width	4.9
Substrate Length	4.9
Substrate Thickness	0.256
Patch Width	2.38
Patch Length	2.38
Patch Height	0.035
Inner Probe Radius	0.30025
Outer Radius	1.0025
Pin offset from the center	0.6

Table 5. Dimensions of the patch antenna parameters

For the design of the patch antenna, the position of the feeding pin in a coaxial fed patch antenna results the most important parameter for impedance matching, radiation pattern, and overall performance of the antenna. Figure 4.4 shows the far-field radiation pattern, showing a gain of 6.5 dBi and a 64 % of radiation efficiency. The feeding pin is located along the center axis of the radiating patch, ensuring therefore vertical polarization, at 0.6 mm below its respective center, offering an impedance matching for the 50 Ohm coaxial connector. The correctness of its position is validated by the results of the reflection coefficient, resulting -26 dB at 31 GHz, as shown in Figure 4.5

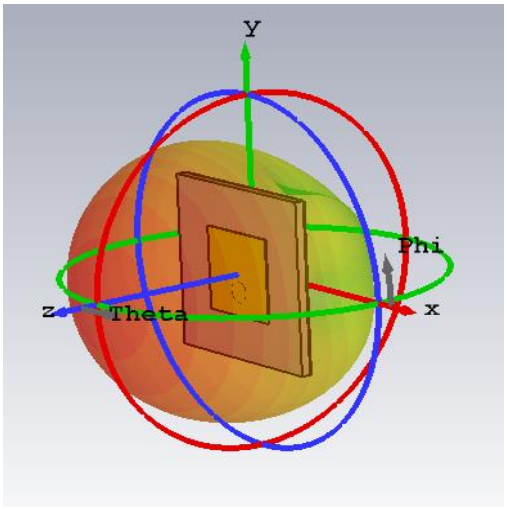

Figure 4.4 - Radiation diagram of the coaxial fed patch

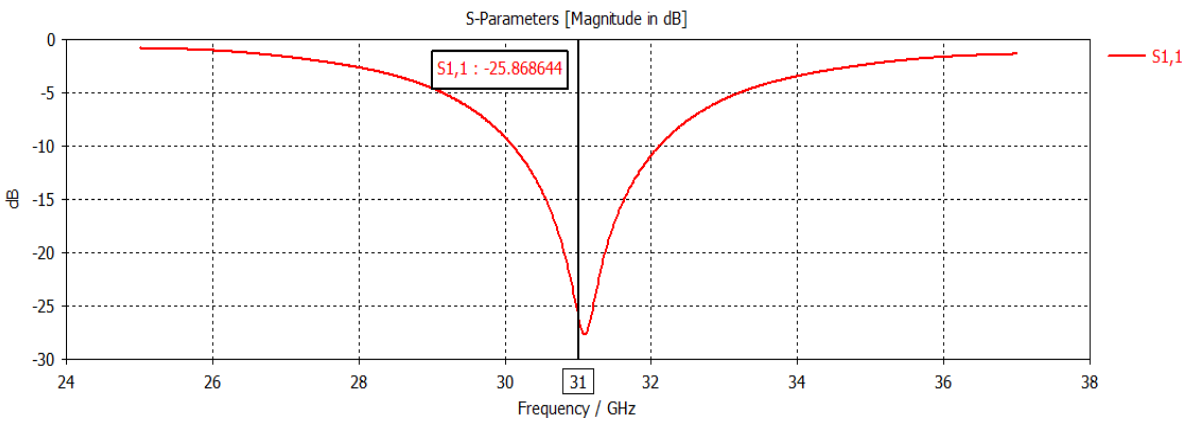

Figure 4.5 S-Parameter centered at resonance frequency.

4.2 Computation of the Area Invested by the Flat-Top Beam

The aim of computing the area dimension of the flat top beam for both configurations is to calculate the number of rectenna systems required to cover it entirely, considering that two patch antennas are spaced by $\frac{\lambda}{2}$. Simple geometrical analysis was used to compute the area invested by the beams at different distances (10cm, 15cm, 20cm. 25cm and 30cm) from the transmitter array. To compute this area invested by the beam only the angular beam width (3dB) was required in the 2 planes i.e. phi = 0° and phi = 90° which were provided by the simulations carried out on CST Studio Suite.

4.2.1 Computation of the Beam Area for Configuration 1 (along rows)

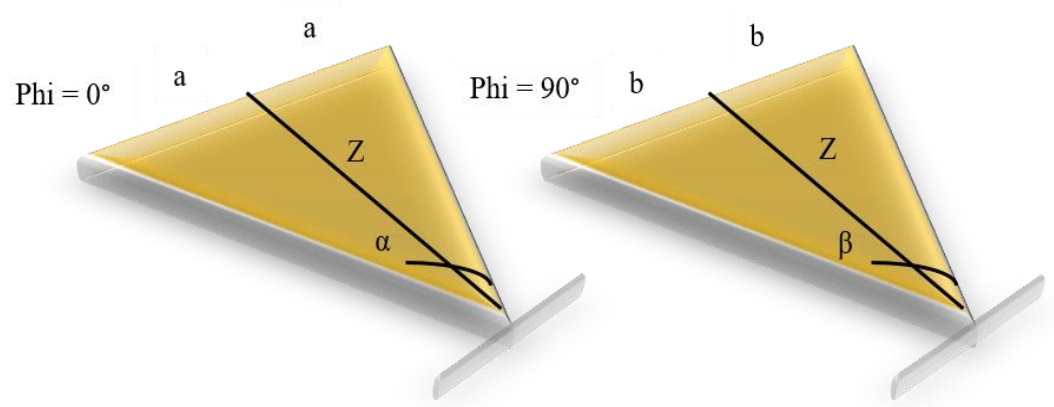

Figure 4.6 Beam pattern depiction to calculate area invested by the beam.

Considering that the area occupied by a single patch (considering its substrate) is $23.52\ mm$, the number of elements required is computed through the following relation:

$$N_{PATCH} = \frac{AREA\ INVESTED\ BY\ THE\ BEAM\ (mm)^2}{AREA\ OF\ THE\ SINGLE\ ELEMENT\ (mm)^2} \qquad (14)$$

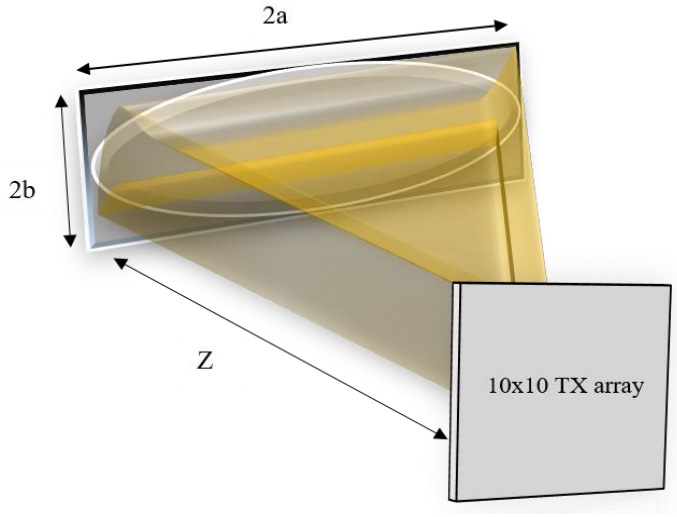

Figure 4.7 Depiction showing that how the beam covers an elliptical area

The method used for computing the number of required elements for the elliptical area invested by the flat-top beam is illustrated in Figure 4.6.

The calculations carried out at all the different distances are summarized in table 6.

Distance (mm)	Area invested (mm^2)	N_{patch}(elliptical)
100	873	28
150	1872	62
200	3840	128
250	5244	175
300	7560	242

Table 6. Summary of the computations carried out to estimate the number of patch antennas

4.2.2 Computation of the Beam Area for Configuration 2D

The area is computed with the same method illustrated before. In this case, the angular beam width in both planes was 23°, therefore the area invested results to be not elliptical anymore, but circular, as depicted in the figure 4.8.

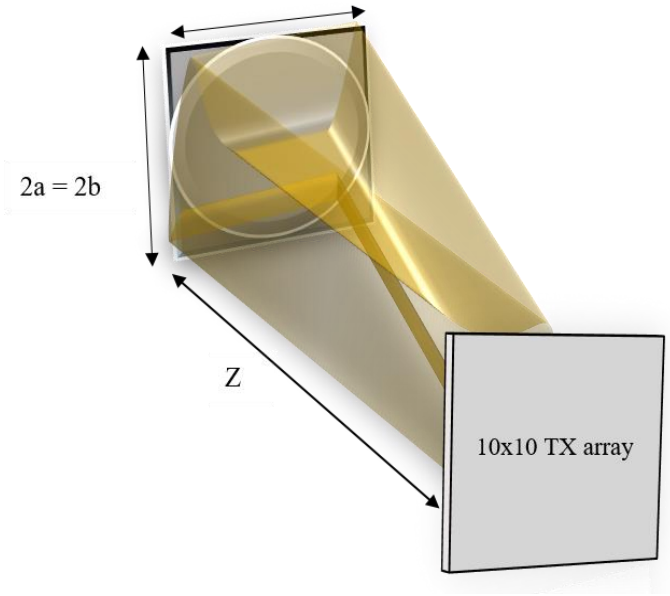

Figure 4.8 Depiction showing that how the beam covers a circular area.

The calculations done below shows that how the number of patch antennas were computed at 10cm from the transmitter array to cover the entire rectangular and circular area. The calculations done at all the different distances are summarized in table 7.

Distance (mm)	Area invested (mm^2)	N_{patch}(circular)
100	1648	55
150	3721	124
200	6561	219
250	10201	340
300	14884	497

Table 7. Summary of the computations carried out to estimate the number of patch antennas (2D)

It can be seen from both table 6 and table 7 that increasing the distance between the transmitter and the receiver increases the area invested and hence the number of patch antenna that could be fitted inside the receiving system.

4.3 Received Power

After estimating the number of patch antennas required to cover the entire area invested by the flat-top beam, power received by every patch for both the configurations was measured using the Friis equation, given by,

$$P_r(dB) = P_t + G_t + G_r + 20log_{10}\frac{\lambda}{(4\pi R)} \qquad (15)$$

Where, Pt is power radiated by the transmitting 10x10 antenna array, Gt is the gain of the transmitting array, Gr is the gain of the receiving patch antenna, and R is the distance between the transmitting array and the receiver. It was noted that each receiving patch experiences a slightly different transmitter gain and hence the received power was slightly different as well, depending on its position. Therefore, for each receiving patch, the contribution of the received power is computed.

4.4 Rectified Power and RF-DC efficiency

As a circuit of reference, in [9], a rectifier circuit is designed and optimized by means of harmonic balance simulations. The matching network, a linear subnetwork that performs impedance matching between the antenna and the rectifier in order to maximize the power transfer flowing into the rectifier, is positioned after the receiving antenna, represented by its Thevenin equivalent circuit. Rectification at mm-Waves is known to be challenging because at high frequencies, package parasitic effects start to matter a lot. The Schottky diode, which is widely utilized in WPT applications, is one type of diode that operates effectively at mm-Waves. Schottky diodes have very fast switching times, making them well-suited for use in high-speed circuits at mm-Wave frequencies and, the forward voltage drop across a Schottky diode is typically lower than that of a p-n junction diode, resulting in less power dissipation and less signal loss in the circuit. The rectifying circuit needs to be adjusted for the input power range, which in this case refers to the power that the antenna receives at various operating distances. The rectifier receives the power that it receives from the antenna as input.

$$Rectification\ Efficiency = \frac{P_{DC}}{P_{IN}} \qquad (16)$$

The RF-DC efficiency is the ratio of the output DC power to the input RF power. It represents the amount of RF power that is successfully converted into usable DC power. In WPT, high RF-DC efficiency is critical to ensure that the available RF energy is effectively converted into usable electrical power. The whole receiving system would work as a DC-combiner. The RF DC efficiency at 31 GHz in response to the input power is presented in Figure 4.9.

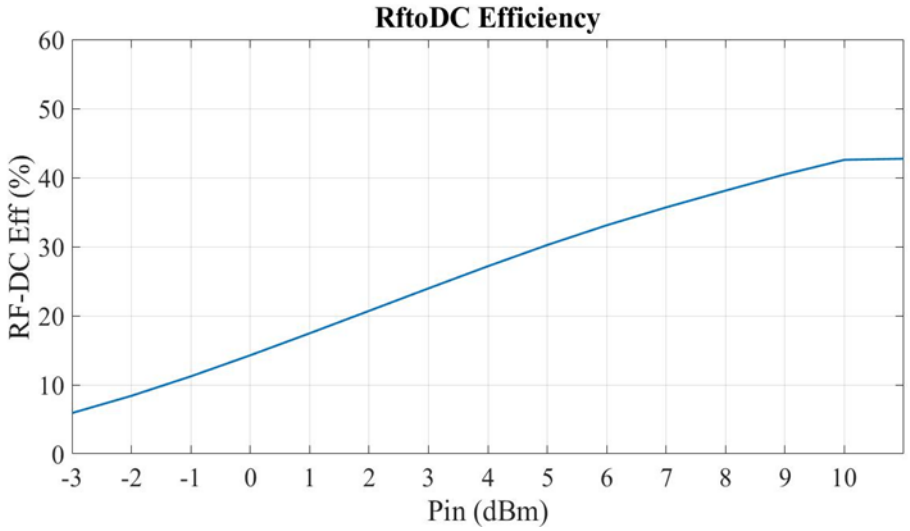

Figure 4.9 Input Power vs RF-DC efficiency curve

5. Results for Measured Received Power and RF-DC Efficiency

In this section, the received power and the RF-DC efficiency for every patch antenna (fitted in the area invested in the two configurations) is computed and the results are listed in tables. At the end, RF-DC efficiency obtained for both configurations are compared and conclusions are made.

5.1 Results for configuration 1 (along rows)

As described in section 4.3, Friis transmission equation was used to find the power received by every patch antenna at the receiver side. For both the configurations, received power in response to the differently experienced transmitted gain was computed at different distances and the resulting RF-DC efficiency was measured for every patch antenna. Then, the total RF-DC efficiency was computed by taking the average. The maximum transmitter gain in all the considered distances was 17.8 dBi.

It must be stated that transmitted power is adjusted in order to have for different distances practically the same average received power that fit in the range of the power that can be handled by the rectifying system. The table below shows the results computed for configuration 1 at five different distances. P_{RX} is the average power received by a single patch, and P_{tot} is the total rectified power by the system, that considers all the DC contributions.

Distance (mm)	P_{TX} (dBm)	P_{RX} / patch (dBm)	N_{patch}	RF-DC Efficiency/patch (%)	P_{tot} (dBm)
100	30	9.78	28	42.5	21
150	34	9.8	62	42	24
200	36	9.1	128	41	26
250	38	9.0	175	40.7	27.5
300	40	9.0	242	40	29

Table 8. Computed results for Configuration 1 (along rows)

5.2 Results for configuration 2D

The maximum transmitter gain for configuration 2D in all the considered distances was 15.8 dBi. For every patch antenna the received power was computed in response to a certain experienced transmitter gain and in return the RF-DC efficiency was measured. The transmitted power was varied according to the power variation in configuration 1 (along rows) in order to have a fair comparison at the end.

It must be stated in this case as well that transmitted power is adjusted in order to have for different distance practically the same average received power that fit in the range of the power that can be handled by the rectifying system.

Distance (mm)	$P_{TX}\ (dBm)$	P_{RX} per patch (dBm)	N_{patch}	RF-DC Efficiency/patch (%)	$P_{tot}\ (dBm)$
100	30	7.8	55	38	22
150	34	7.5	124	38	24.2
200	36	7.2	219	37	26.2
250	38	7.3	340	36.6	28.2
300	40	7.1	497	36	29.5

Table 9. Computed results for Configuration 2D

5.3 Comparison between configuration 1(along rows) and 2D Performance

Table 10 compares the results obtained in terms of received power and RF-DC efficiency for both configuration 1(along rows) and 2D, where P_{RX} is the power received by a single patch, and P_{tot} is the total rectified power by the system. It can be concluded from table 9 that, as the distance from the transmitter array increases, the average received power received by a single patch element decreases . Configuration 1 provides better results in terms of average RF-DC efficiency per patch, whereas, Configuration 2D gives better results in terms of total rectified power even though the transmitter gain in case of configuration 2D was less compared to configuration 1. If the power transmitted in case of configuration 2D is increased then surely, the total rectified power would be much higher compared to the rectified power obtained in case of configuration 1. Therefore, it can be concluded that, configuration 2D is a better scheme

in terms of total rectified power and also configuration 2D allows to cover a larger area and more number of receiving antennas can be accumulated.

Distance	150 mm	200 mm	250 mm	300 mm
Configuration 1(along rows)	P_{TX} = 34 dBm	P_{TX} = 36 dBm	P_{TX} = 38 dBm	P_{TX} = 40 dBm
	P_{RX} = 9.8 dBm	P_{RX} = 9.1 dBm	P_{RX} = 9.0 dBm	P_{RX} = 9.0 dBm
	P_{tot} = 24 dBm	P_{tot} = 26 dBm	P_{tot} = 27.5 dBm	P_{tot} = 29 dBm
Configuration 2D	P_{TX}= 34 dBm	P_{TX}= 36 dBm	P_{TX} = 38 dBm	P_{TX} = 40 dBm
	P_{RX}= 8.19 dBm	P_{RX} = 7.52 dBm	P_{RX}= 7.3 dBm	P_{RX} = 7.1 dBm
	P_{tot} = 24.2	P_{tot} = 26.2	P_{tot} = 28.2	P_{tot} = 29.5

Table 10. Comparison between configuration 1(along rows) and 2D.

Conclusion

In this thesis, a numerical investigation for a special type of array called flat-top beam arrays has been carried out to enhance the RF-DC efficiency in WPT scenarios. In chapter 2, a detailed analytical analysis of the antenna arrays has been provided, discussing the main antenna terminologies with formulation and their types.

Chapter 3 describes the design of the 10x10 planar flat-top dipole array and how the flat-top beam was achieved. Starting from a single dipole antenna, the array was scaled to a size of 10x10, and its performance was optimized through extensive simulations. The flat-top beam was achieved through amplitude and phase control which involved adjusting the amplitude and phase of the signal that was fed into each antenna element in the array. By carefully controlling the amplitude and phase of each signal, it was possible to create a flat-top beam that had a uniform energy distribution across its width. After successfully creating the flat-top beam, it was noticed that the flat beam was larger horizontally but a bit smaller vertically because the amplitude and phases were applied horizontally (row by row), this was called configuration 1 (along rows). Therefore, a second method called configuration 2D was tested in which the amplitude and phases were applied to each antenna element in a 2-dimensional way. This created a flat-top beam that was symmetrical both horizontally as well as vertically. Along the process, multiple tests were run to improve the flatness of the beam and a better flatness was acquired but a trade-off was found between better flatness and higher SLL.

Chapter 4 focuses on the receiver side to measure the RF-DC efficiency. A single coaxial-fed patch antenna was designed, and its performance was optimized. As the flat-top beam offers a better power distribution on the receiving surface hence, the beam area was computed by using geometric analysis, and the number of patch antennas that would fill the computed area was calculated for both configurations. Every receiving antenna had its own rectifying circuit i.e. every antenna was acting as a rectenna and the aim was to calculate the power received by every patch antenna at different distances from the 10x10 flat-top beam array using the Friis equation. The RF-DC efficiency vs received power curve was used to calculate the efficiency for every patch antenna in the system that covered the beam area.

Finally, in chapter 5, all the results related to the total efficiency of the receiving system has been compiled w.r.t to power received through both configurations at different distances. It was found that because of flat-top beam, every patch antenna was receiving almost constant power which resulted in high RF-DC efficiency. There was a slight variation in the received power and hence the efficiency when the distance between the transmitter and the receiving

system kept on increasing but still, the average efficiency per patch was more than acceptable. In comparison it was found that the configuration 1(along rows) provides better results in terms of average RF-DC efficiency per patch whereas, configuration 2D produced better results in terms of total rectified power even though the transmitted gain was less as compared to configuration 1. This was because in configuration 2D the flat-top beam covered a 2-dimensional area and covered a large number of receiving patch antennas. By increasing the transmitted power in case of configuration 2D, even better rectified power could be achieved. Therefore, it can be concluded that flat-top beam array plays a vital role in improving the RF-DC efficiency of WPT scenarios such as wireless charging of electronic devices, remote powering of sensors, and wireless power transfer in space-based applications. Overall, the use of flat-top beams is an important technology that can significantly improve the efficiency and effectiveness of wireless power transfer systems.

References

[1]: Wireless Power Transfer—A Review Kalina Detka and Krzysztof Górecki * Department of Marine Electronics, Faculty of Electrical Engineering, Gdynia Maritime University, Morska 83, 81-225 Gdynia, Poland

[2] “Antennas for Wireless Systems” notes of the lectures of the course of A.A. 2020-21

[3]: Array Pattern Synthesis of Flat-topped Beam for Microwave Power Transfer System at Volcanoes. Nobuyuki Takabayashi∗, Naoki Shinohara∗ and Teruo Fujiwara† ∗Research Institute for Sustainable Humanosphere, Kyoto University Gokasho, Uji, Kyoto, Japan 611-0011 †Sho Engineering Corp. 2-14-9, Takanawa, Minato-ku, Tokyo, Japan 108-0074

[4]: An Effective Sandwiched Wireless Power Transfer System for Charging Implantable Cardiac Pacemaker. Chunhua Liu , Senior Member, IEEE, Chaoqiang Jiang , Student Member, IEEE, Jingjing Song , and K. T. Chau , Fellow, IEEE

[5]: C. Balanis, Antenna Theory: Analysis and Design. John Wiley, 1997.

[6]: Flat-topped beam forming experiment for microwave power transfer system to a vehicle roof. Takaki ishikawa and Naoki shinohara Wireless Power Transfer, 2015, 2(1), 15–21. # Cambridge University Press, 2015

[7]: DESIGN AND REALIZATION OF A FLAT-TOP SHAPED-BEAM ANTENNA ARRAY H. J. Zhou, Y. H. Huang, B. H. Sun, and Q. Z. Liu National Key Laboratory of Antennas and Microwave Technology Xidian University Xi’an, Shaanxi 710071, China

[8]: R. Visintini Elettra Synchrotron Light Laboratory, Trieste, Italy

[9]: PRECISE NEAR-FIELD FOCUSING EXPLOITING BESSEL BEAM LAUNCHERS FOR WIRELESS POWER TRANSFER AT MILLIMETER WAVES, Augello Elisa Chiar.ma Prof. Alessandra Costanzo, 2020/21.

List of Tables